의학박사 학위논문

Intracarotid Injection of Adipose Tissue-originated Platelet-Derived Growth Factor Receptor β-positive Cells in Rat and Canine model: Feasibility of Cell Delivery under Mannitol-induced Blood-Brain Barrier Opening

백서와 개모델에서 지방조직유래 혈소판성장인자 베타수용체 양성 세포의 경동맥 주입 방법 연구: 고장성 만니톨 주입으로 유도된 혈액-뇌장벽 해제 후 세포 전달의 유용성

2012년 8월

서울대학교 대학원
의학과 뇌신경과학 전공
윤 성 원

의학박사 학위논문

Intracarotid Injection of Adipose Tissue-originated Platelet-Derived Growth Factor Receptor β-positive Cells in Rat and Canine model: Feasibility of Cell Delivery under Mannitol-induced Blood-Brain Barrier Opening

백서와 개모델에서 지방조직유래 혈소판성장인자 베타수용체 양성 세포의 경동맥 주입 방법 연구: 고장성 만니톨 주입으로 유도된 혈액-뇌장벽 해제 후 세포 전달의 유용성

2012년 8월

서울대학교 대학원

의학과 뇌신경과학 전공

윤 성 원

Intracarotid Injection of Adipose Tissue-originated Platelet-Derived Growth Factor Receptor β-positive Cells in Rat and Canine model: Feasibility of Cell Delivery under Mannitol-induced Blood-Brain Barrier Opening

지도 교수 노 재 규

이 논문을 의학박사 학위논문으로 제출함.

2012년 8월

서울대학교 대학원

의학과 뇌신경과학 전공

윤 성 원

윤성원의 의학박사 학문논문을 인준함.

2012 년 8 월

위 원 장 _____

부위원장 _____

위 원 _____

위 원 _____

위 원 _____

Intracarotid Injection of Adipose Tissue-originated Platelet-Derived Growth Factor Receptor β-positive Cells in Rat and Canine model: Feasibility of Cell Delivery under Mannitol-induced Blood-Brain Barrier Opening

by Sung Won Youn

A thesis submitted in partial fulfillment of the requirement for the degree of Doctor of Philosophy in Medicine (Neuroscience)

at the Seoul National University College of Medicine

June 2012

Approved by thesis committee

Professor _____ Chairman

Professor _____ Vice Chairman

Professor _____

Professor _____

Professor _____

학위논문 원문제공 서비스에 대한 동의서

본인은 본인의 연구 결과인 학위논문이 앞으로 우리나라의 학문발전에 조금이나마 기여 할 수 있도록, 서울대학교 중앙도서관을 통한“학위논문 원문제공 서비스”에서 다음과 같은 방법 및 조건하에 논문을 제공함에 동의합니다.

1. 인터넷을 통한 온라인 서비스와 보존을 위하여 저작물의 내용을 변경하지 않는 범위내에서의 복제를 허용함.
2. 저작물을 이미지DB (PDF)로 구축하여 인터넷을 포함한 정보통신망에서 공개하여 논문 일부 또는 전부의 복제·배포 및 전송에 동의함.
3. 해당 저작물의 저작권을 타인에게 양도하거나 또는 출판허락을 하였을 경우 1개월 이내에 서울대학교 중앙도서관에 알림.
4. 배포, 전송된 학위논문은 이용자가 다시 복제 및 전송할 수 없으며 이용자가 연구목적이 아닌 상업적 용도로 사용하는 것을 금함에 동의함.

논문제목

Intracarotid Injection of Adipose Tissue-originated Platelet-Derived Growth Factor Receptor β-positive Cells in Rat and Canine model: Feasibility of Cell Delivery under Mannitol-induced Blood-Brain Barrier Opening

학 과(부) : 의 학 과

학 번 : 2005-30694

연 락 처 :

제 출 일 : 2012년 7월

저 작 자 : 윤 성 원 (인)

Abstract

Adipose tissue-originated pericyte with platelet-derived growth factor receptor β positivity (AT-PDGFRβ$^+$) is a multipotential mesodermal stem cell which is promising for a cell-based neurorestorative therapy. The current study of chronic ischemic rat model was conducted to test whether hyperosmolar mannitol enhances intracarotid delivery of AT-PDGFRβ$^+$ cells and to investigate whether contralaterally infused AT-PDGFRβ$^+$ cells would reach ischemic hemisphere and differentiate into neuronal or endothelial cells. The safety of the intracarotid injection of hyperosmolar mannitol and autologous AT-PDGFRβ$^+$ cells was additionally tested for a non-ischemic normal canine model. For the chronic ischemic rat model, 1.4M mannitol (2mL, 0.1mL/sec) and $2x10^6$ human AT-PDGFRβ$^+$ cells (n=9), or injection of $2x10^6$ human AT-PDGFRβ$^+$ cells alone (n=6) were infused in the contralateral carotid artery at three weeks after ischemia. AT-PDGFRβ$^+$ cells were found in the non-ischemic hemisphere and the corpus callosum at

day 3, and in the ischemic hemisphere at day 7 under the condition of mannitol pretreatment. However, without mannitol pretreatment, only a few AT-PDGFRβ$^+$ cells were observed in the infarct areas at day 7. At day 28, the surviving AT-PDGFRβ$^+$ cells in the ischemic hemisphere were located mainly in the perivascular space, and were immunostained with endothelial barrier antigen (EBA; ~65%), alpha smooth muscle actin (αSMA; ~40%) or neurofilament (~20%). Normal canines (25kg, n=6) underwent intracarotid injection of hyperosmolar mannitol (20%, 50mL, 1g/kg) followed by 5x10^6 autologous AT-PDGFRβ$^+$ cells. In the original protocol (protocol 1, n=2), cells mixed with 2mL of normal saline were infused for 1 minute by hand injection. In the modified protocol (protocol 2, n=4), cells mixed with 50mL of normal saline and 1,000 unit of heparin, were dripped slowly during 10 minute. During the procedure, vital signs of mean arterial pressure, heart rate, and O_2 saturation were stable. On blood test, the level of leukocyte, hematocrit, calcium, potassium, albumin and total protein was decreased, but the other

blood count, electrolyte, liver and renal batteries were within normal range including CRP. Although all canines were free from neurologic deficit and showed arterial patency on serial angiogram, brain MRI demonstrated multiple ischemic lesions in one canine (protocol 1; 1 out of 2) and a single transient small ischemic lesion in one canine (protocol 2; 1 out of four). In canine brain sections, AT-PDGFRβ^+ cells were detected in both ipsilateral and contralateral cortex, which was more frequent at ipsilateral and frontal location. AT-PDGFRβ^+ cells were also detected within infarcted area, and their location was perivascular spaces (70%), outside vessels (20%), and within vessels (10%), regardless of infracted area or not. In summary, hyperosmolar mannitol enhanced the entrance of contralaterally infused human AT-PDGFRβ^+ cells into chronic ischemic rat brain by transient opening of blood-brain-barrier, and human AT-PDGFRβ^+ cells subsequently migrated across corpus callosum into the ischemic hemisphere and differentiated into neuronal or endothelial cells. The intracarotid injection of autologus

AT-PDGFRβ^{+} cells in normal canines did not develop serious adverse events except for silent thromboembolism. To reduce the thromboembolic complication, additional modification is required for cell pellet concentration. The intracarotid infusion of AT-PDGFRβ^{+} cells under the hyperosmolar mannitiol pretreatment is a feasible therapeutic approach in chronic stroke.

Key words: pericyte, adipose tissue-originated platelet-derived growth factor receptor β-positive (AT-PDGFRβ^{+}) cells, chronic ischemia, rat, canine, intracarotid injection, hyperosmolar mannitol, blood-brain barrier

Student number: 2005-30694

List of Tables

List of Figures

List of abbreviation

ATSC (adipose tissue-originated stromal cell)

AT-PDGFRβ^{+} (adipose tissue-originated platelet-derived growth factor receptor β positive)

BBB (blood-brain barrier)

MACS (magnetic-activated cell sorting)

DMEM (Dulbecco's Modified Eagle Medium)

FBS (fetal bovine serum)

PBS (phosphate buffered solution)

GFP (green fluorescent protein)

EBA (endothelial barrier antigen)

αSMA (alpha smooth muscle actin)

CRP (C-reactive protein)

ICA (internal carotid artery)

Contents

I. INTRODUCTION

Stroke remains the second leading cause of death and the leading cause of adult disability in industrialized countries including Korea (1–3). About 30%–50% of stroke survivors remain independent and 15%–30% are severely disabled. Numerous neuroprotective attempts have been made to interrupt the ischemic cascades (4). Despite the promising results from in vitro and animal experiments, all clinical trials failed to demonstrate the efficacy of neuroprotective therapy (5). Recently the enormous potentials of stem or progenitor cells for cell-based neuroregeneration have been recognized (6–11). Several studies suggested that stem or progenitor cells harvested from bone marrow (6,10,12), peripheral blood (13-15), cord blood (16), and adipose tissue (17–20) can exhibit neuronal or glial cell properties, or secrete cytokines and neurotrophic factors under specific culture conditions. From adipose tissue, the stem or progenitor cells can be harvested more easily and abundantly than

other sources, and adipose tissue-originated stromal cell (ATSC) can produce pericytes or its precursor cells (21–25).

It has been suggested that pericytes, which are originally defined by their morphology and close contact to endothelial cells (26–29), may have function as multipotent mesodermal stem cells (MSCs) for tissue repair (22–25). Although no single specific marker is available to define the pericyte phenocyte, platelet-derived growth factor receptor β (PDGFRβ), α-smooth muscle actin (αSMA) or chondroitin sulfate proteoglycan NG2 have been used to identify pericytes (23,24,30–33). Pericytes can differentiate into mature pericytes, osteoblasts, chondroblasts, fibroblasts, adipocytes, and smooth muscle cells (23,32,34–38). In addition, pericytes may be a source of MSCs with the potential of direct vasculo-neurogenesis (24), and can be useful for future therapeutic strategies.

However, a cell-based therapy for acute stroke should overcome two major obstacles in the clinical application. First, two or three

weeks are required for expanding autologous stem cells isolated from patient's tissue to obtain sufficient amount for infusion. During the elapsed time of expansion, acute stroke evolves to subacute stage, with losing homing signals for stem cells recruitment and blood-brain barrier (BBB) being closed. The BBB disruption would be a prerequisite for entering brain tissue at this situation. In this study, we hypothesized that transient BBB disruption with hyperosmolar mannitol would enhance stem cell delivery at subacute or chronic stage of stroke. Second, intracarotid administration has an advantage over the other route of administration, but arrested flow through occluded artery may not be effective to deliver stem cells to brain parenchyma. An arterial infusion through intact contralateral carotid may be more effective for delivery, but it is questionable whether migration of stem cells into ischemic hemisphere would occur.

The current study of chronic ischemic rat model was conducted to

test the hypothesis that hyperosmolar mannitol improves the efficacy of intracarotid delivery of adipose tissue-originated pericyte with platelet-derived growth factor receptor β positive (AT-PDGFRβ^{+}) and to investigate whether AT-PDGFRβ^{+} cells infused contralaterally to ischemic hemisphere would reach cerebral ischemic lesions and differentiate into neuronal or endothelial cells. In addition, non-ischemic normal canine model was carried out to further test the safety of intracarotid infusion of hyperosmolar mannitol and autologous AT-PDGFRβ^{+} cells.

II. METHODS

1. Experimental design and animal groups

1.1. Treatment allocation of chronic ischemic rat

Chronic ischemic rats were allocated to either an intracarotid 1.4M mannitol (2mL, 0.1mL/sec) pretreatment group (n=9) or a control group (n=6) infused with 200 μL steril phosphate buffered solution (PBS). Both groups received intracarotid infusion of $2x10^6$ human AT-PDGFRβ^+ cells.

1.2. Normal canines

All normal non-ischemic canines (25kg, n=6) underwent intracarotid injection of hyperosmolar mannitol (20%, 50cc, 1g/kg) followed by $5x10^6$ autologous AT-PDGFRβ^+ cells.

2. Preparation of AT-PDGFRβ^+ cells

2.1. Human adipose tissue acquisition for rat

experiment

Human subcutaneous adipose tissue was acquired from three female subjects (age: 35, 44, 50 years) who underwent an elective surgery. Informed consent for each patient was obtained and the study protocol was approved by the institutional review board of Seoul National University Hospital. As previously described (22), tissues obtained from the patients were transported to our laboratory in PBS containing antibiotics. Tissues were washed at least three times with PBS to remove blood and then digested with 0.075% collagenase type 1 (Worthington Biochemical, Lakewood, NJ, USA) for 1 h at 37 °C. Mature adipocyte fractions were removed from stroma-vascular fractions by centrifuging at 1200×g for 10 min. The remaining fractions were treated with red blood cell lysis buffer for 10 min at room temperature and then filtered through 100-μm nylon mesh to exclude remaining erythrocyte debris, and then recentrifuged at 1200×g for 10min. Stroma-vascular fractions

were utilized for our experiment.

2.2. Autologous canine adipose tissue acquisition for canine experiment

Canine adipose tissues were directly obtained for individual canines. After removing mature adipocyte fractions and red blood cells by the same method of adult human adipose tissue preparation, stroma-vascular fractions were utilized for our experiments. Tissue samples were subjected to long-term culture after magnetic-activated cell sorting (MACS) to obtain adequate number for transplanatation.

2.3. Magnetic-activated cell sorting

Approximately 2 x 10^7 cells were incubated with endothelial growth media (EGM-2; Clonetics, San Diego, CA, USA) for 1 h. The cells were then washed with PBS / 5% fetal bovine serum (FBS) and

resuspended in a 1/50 dilution of anti-human PE-PDGFRβ for 45 minutes on ice. After washing, the cells were incubated with anti-PE microbeads (Miltenyi Biotec, Bergisch Gladbach, Germany) for 15 minutes on ice and then separated on a Mini MACS magnetic column (Miltenyi Biotec, Auburn, CA, USA) according to the manufacturer's recommendations.

2.4. Long-term culture and proliferation of AT-PDGFRβ^{+} cells

AT-PDGFRβ^{+} cells sorted by MACS were plated at a density of 1~2x10^{4} per well on 2% gelatin (Sigma)-coated 100mm plates. Cells were maintained under the media condition, DMEM / F12 + 5% FBS + N2 supplement without growth factors, which allowed the cells to maintain their PDGFRβ positivity in our previous study (data are not shown; 21).

3. Intracarotid injection of AT-PDGFRβ$^+$ cells

For the cell tracking study, AT-PDGFRβ$^+$ cells were infected with Lenti-green fluorescent protein (GFP) virus (10^7 plaque-forming units/mL medium) overnight and cultured for additional 2 days before transplantation

3.1. Rat model

At 3 weeks post-ischemia, anesthesia was reinstituted and a modified polyethylene catheter was inserted into the external carotid artery (ECA) toward the bifurcation. The silk tie was tightened around the catheter, and hyperosmolar mannitol solution was injected (1.4 M bolus in saline, 0.1 mL per sec, 2 mL). Five minutes later, approximately 2 x 10^6 AT-PDGFRβ$^+$ cells in 200 μL of PBS was slowly injected over 5 minutes (n=9). A control experiment was conducted using an identical protocol and injecting 2 mL of sterile PBS followed by infusion of 2 x 10^6 AT-PDGFRβ$^+$ cells in 200 μL of PBS over 5 minutes (n=6). All animals were not treated with

immunosuppressants in this study.

3.2. Canine model

Since chronic ischemic rat experiments demonstrated the enhanced penetrance of AT-PDGFRβ^{+} cells with hyperosmolar mannitol pretreatment, all canine experiments were conducted with hyperosmolar mannitol pretreatment. All canines were fasted from the night before procedures. Using a femoral approach, carotid angiogram was obtained by using 5F Davis catheter (Jungsung medical, sungnam-si, Korea) under inhaled anesthesia. To prevent clot formation within catheter, continuous heparin-saline pressure bag was connected to 5F catheter. To open the BBB, hyperosmolar mannitol solution (20% mannitol, total 50cc, 1g/kg, for 1 minute) was infused through microcatheter positioned at internal carotid artery. Post-mannitol injection angiography was obtained to confirm arterial patency. In the original protocol (protocol 1, n=2),

approximately 5 x 10^6 autologous AT-PDGFRβ^+ cells in 2mL of PBS was slowly injected by hand injection 5 minutes after mannitol pretreatment. After experiencing a thromboembolic complication, we modified the infusion protocol (protocol 2). In the protocol 2 (n=4), cell solution was dissociated with hand shaking after addition of EDTA/Trypsin. Autologous AT-PDGFRβ^+ cells were mixed with a 50 mL of normal saline plus 1,000 unit of heparin solution, and the mixture were dripped slowly using pressure bag during 10 minute. Blood pressure, heart rate, and EKG were monitored at baseline, 1 minute and 5 minutes after mannitol injection, and 10, 15, and 30 minutes after cell injection. Post-PDGFRβ^+ injection angiography was obtained to assess arterial patency.

4. Brain magnetic resonance imaging for canines

Anesthesia was adjusted to maintain immobility during MRI scan. Using a 3.0 Tesla scanner (Magnetom Vision, Siemens, Erlangen,

Germany), T1- and T2-weighted images, fluid-attenuated inversion recovery (FLAIR), diffusion-weighted images of sagittal, transversal, or dorsal planes were obtained. Infarct area was defined as increased intensity greater than a factor of 1.25 as compared to normal area. The presence of embolic infarct was examined at 1 day and 1 week after AT-PDGFRβ^+ cell injection.

5. Neurobehavioral scoring for canines

Neurobehavioral scoring was performed using a standardized categorical rating scale (39–41); scoring was performed for motor function (no deficit= 1, hemiparetic but able to walk = 2, stands only with assistance = 3, hemiplegic and unable to stand = 4, comatose or dead, not testable = 4), consciousness (normal = 1, mildly reduced = 2, severely reduced = 3, comatose or dead= 4), head turning (absent = 0, posturing and turns toward side of infarct = 1, unable to lift head, comatose, or dead =1), circling (absent =

0, present = 1, does not walk or dead= 1), and hemianopsia (absent = 0, present = 1, unable to test because of reduced consciousness or death = 1). Total neurobehavioral score ranges from 2 (completely normal) to 11 (most severe deficits: comatose or dead). Each canine was assessed prior to anesthesia, daily during the first week, and then weekly until euthanasia.

6. Blood Sample Collection for canine

Blood samples were taken prior to, 1 day after, and 1 week after intracarotid injection; A total of 5–10 mL blood was collected into ethylene diaminetetraacetic acid (EDTA) tubes and was sent for a complete blood cell count (CBC), liver and renal battery, coagulation study, and arterial blood gas analysis.

7. Immunocytochemistry for brain tissues

Rats were sacrificed for immunohistochemistry at 3, 7, and 28

days after AT-PDGFRβ^{+} cell transplantation. Canines were euthanized at 28 days after transplantation. After 24 hours of fixation in 4% paraformaldehyde, brains were cryoprotected with 30% sucrose for 24 hours and then cut into 30 μm sections with a cryostat (Leica CM 1900; Leica, Deerfield, IL). Brain sections were fixed for 30 minutes at room temperature in 4% paraformaldelyde and then washed 3 times in PBS. To examine the phenotypic differentiation of transplanted cells, brain sections were stained with anti-GFP antibody and antibodies against different cell markers of neuron, pericyte, and endothelial cell. Sections were labeled with chicken anti-GFP (1:800, Abcam), and either anti-Nestin (1:200, Chemicon), anti-PDGFRβ (1:200; Abcam), anti-NG2 antibodies (1:100; Abcam); anti-αSMA antibodies (1:100; DAKO); anti-NF (1:200, Chemicon), and anti-endothelial barrier antigen (EBA) (1:200; Stenberger Monoclonals, Baltimore, MD, USA) antibodies. FITC-conjugated anti-sheep IgG (1:100; Biodesign) and Cy3-

conjugated anti–mouse IgG antibodies (1:300; Jackson Immunoresearch Laboratories) were used as secondary antibodies. Negative controls were generated by adding the same concentration of primary mouse IgG (Sigma) or sheep IgG (#I5006; Sigma). Fluorescence signals were detected at excitation/emission wavelengths of 550/570nm (Cy3, red), 488/522nm (FITC, green), and 360/400nm (DAPI, blue). Images were then acquired on a Bio-Rad MRC 1024 inverted confocal microscope (Bio-Rad).

7. Statistical analysis

Data of continuous variables were expressed as means ± standard deviations. The Pearson's chi-square test was used to compare the frequency distributions of categorical variables between the study groups. Continuous variables were compared using Student's t test, the Mann-Whitney U test, or Kruskal-Wallis test. P-value < 0.05 was considered statistically significant.

III. RESULTS

1. Preparation of AT-PDGFRβ^{+} cells

The AT-PDGRβ^{+} cells obtained from human and canine adipose tissue were analyzed by using flow cytometry. They were sorted by high PDGFRβ expression and lack of CD34, the latter in order to ascertain the absence of endothelial cells within sorted cells. The cells formed a monolayer of homogenous bipolar spindle-like cells with a whirlpool-like array within 2 weeks (Fig 1A). The light microscopy analysis demonstrated that these cells maintained a stable morphology and immunophenotype for PDGFRβ for about 25 to 30 passages in culture without spontaneous differentiation. The stable proliferation of AT-PDGFRβ^{+} without differentiation into mature pericytes was achieved at condition of DMEM / F12 + 5% FBS + N2 supplement without growth factors (Fig 1B).

(A) (B)

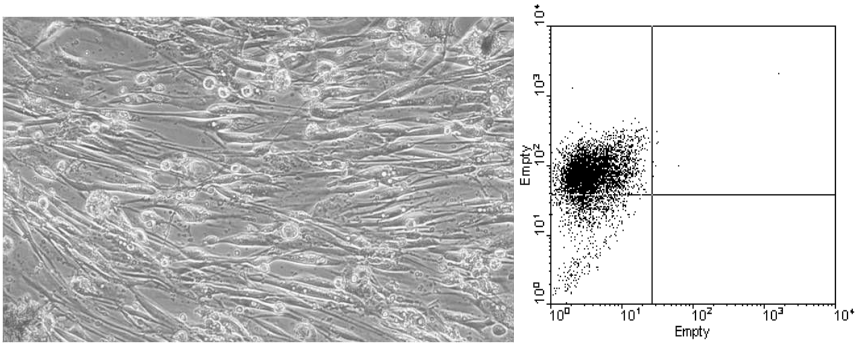

Figure 1. Isolation and culture of PDGFRβ^{+} cells sorted from adipose tissue and flow cytometry analysis

(A) The PDGFRβ^{+} cells were sorted from adipose tissue and seeded in culture. The cells formed a monolayer of homogenous bipolar spindle-like cells with a whirlpool-like array within 2 weeks. (B) Cell suspensions from adipose tissues were stained with PDGFRβ antibodies and run on a flow cytometry analysis. The majority (about 98%) of cell suspensions were positive for PDGFRβ by flow cytometry at condition of DMEM / F12 + 5% FBS + N2 supplement without growth factors.

2. Identification and trafficking of transplanted human AT-PDGFRβ$^+$ cells within rat brain

At three weeks after ischemia, the Lenti-GFP-transfected AT-PDGFRβ$^+$ cells were injected through the contralateral internal carotid artery with hyperosmolar mannitol pretreatment. After sacrifice of rats, brain sections were stained at day 3, day 7, day 28 for expression of GFP. When human AT-PDGFRβ$^+$ cells were infused at contralateral carotid artery, the GFP$^+$ cells were found in the non-ischemic hemisphere (injected side) and the corpus callosum at day 3 (Fig 2A,B). The GFP$^+$ cells began to be found in the ischemic hemisphere at day 7 (Fig 2C,D). Therefore, the GFP$^+$ cells migrated into the ischemic hemisphere via corpus callosum at day 7. The transplanted cells showed positivity for both GFP and nestin around the ischemic core 7 days after injection (Fig 2D–F).

Brain sections on day 28 were stained with antibody for GFP, EBA, αSMA, and NF (Fig 2G–O). The surviving GFP$^+$ cells in the ischemic

brain were located mainly in the perivascular space, as indicated in EBA immunostaining (~65%). They expressed a pericyte marker, αSMA (~40%) or a neuronal marker, NF (~20%). Astroglial differentiation of transplanted cells was not observed at 7 or 28 days after transplantation.

However, in cases with contralateral injection without mannitol (Fig 2P,Q) or with ipsilateral injection with mannitol (Fig 2R), there were only a few GFP^+ cells in the infarct areas at day 7.

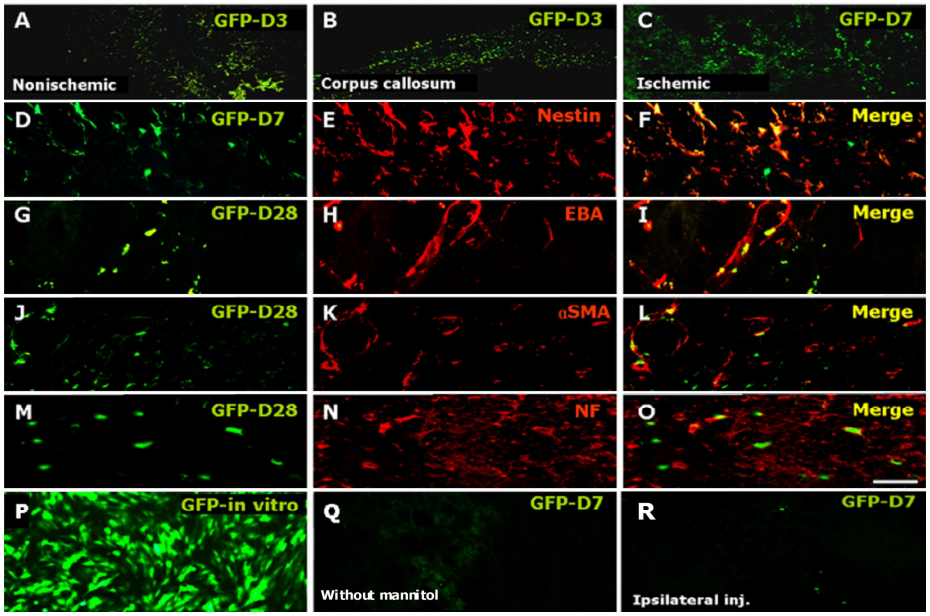

Figure 2. Migration and differentiation of transplanted AT-PDGFRβ$^+$ cells in chronically ischemic rat brain

The GFP$^+$ cells were found not only in the injected non-ischemic hemisphere (A), but also in the corpus callosum (B) on day 3 after injection. The GFP$^+$ cells migrated and distributed to a large area in the ischemic hemisphere on day 7 (C). Most GFP$^+$ cells were nestin-positive (D-F). Brain sections on day 28 were stained with antibody for GFP, EBA (G-I), αSMA, and NF. The majority of the GFP$^+$ cells was located in the perivascular space and expressed αSMA (J-L),

whereas some expressed NF (M-O). (P) The Lenti-GFP-transfected AT-PDGFRβ^{+} cells are shown as green fluorescent color. (Q) In case of contralateral cell infusion without hyperosmolar mannitol pretreatment, there were only a few GFP-positive cells in the infarct areas at day 7. (R) In case of ipsilateral cell infusion with hyperosmolar mannitol pretreatment, there were only a few GFP-positive cells in the infarct areas at day 7. Scale bar represents 30 μm in D-O.

3. Safety of intracarotid injection of autologous AT-PDGFRβ$^+$ cells in normal canine

Serial common carotid angiogram of six canines after autologous AT-PDGFRβ$^+$ cell injection showed arterial patency without evidence of thromboembolic occlusion (Table 1). At each step of the procedure, vital signs of mean arterial pressure, heart rate, and O_2 saturation remained stable ($p>0.05$; Table 2). On blood test, the leukocyte count, serum calcium, serum potassium, total protein and albumin levels were decreased after infusion as compared to baseline ($p<0.05$; Table 3), but the other blood count, electrolyte, liver, renal and coagulation batteries were within normal range. The C-reactive protein (CRP) was within normal range. On neurological scales, all six canines showed intact motor and consciousness (Table 4). Abnormal movements of head turning, circling, and hemianopsia were not observed. Brain MRIs of 1 day and 7 days showed acute infarct in two canines, and the incidence of acute infarct was 50%

with the protocol 1 and 25% with the protocol 2 (Table 5); in canine#1, small areas of diffusion-restriction was found on frontal lobe contralateral to injected side at 1 day DWI, and on ipsilateral temporoparietal lobe at 1 week FLAIR (Fig 4). Canine#5 showed a tiny lesion at 1 day, which disappeared in the follow-up FLAIR images performed at day 7 (Fig 5).

Table 1. Angiographic findings of six canines after intracarotid injection of autologous AT-PDGFRβ^{+} cells

Canine No.	ACA	MCA
Canine No.1	No occlusion	No occlusion
Canine No.2	No occlusion	No occlusion
Canine No.3	No occlusion	No occlusion
Canine No.4	No occlusion	No occlusion
Canine No.5	No occlusion	No occlusion
Canine No.6	No occlusion	No occlusion

AT-PDGFRβ^{+}=adipose tissue-originated platelet-derived growth factor receptor β positive cell; No.=identification number; ACA=anterior cerebral artery; MCA=middle cerebral artery

Table 2. Arterial pressure, heart rate, and SpO_2 at baseline, immediate post-infusion, day 1, and day 7 after AT-PDGFRβ$^+$ cell infusion

	MAP, mmHg	HR, beats/min	SpO_2, %
baseline	117.3±4.8	85.5±6.7	99.8±0.4
1min manitol	120.5±2.3	85.3±6.1	99.8±0.4
5min manitol	119.7±2.7	83.5±5.2	100±0
10min AT-PDGFRβ$^+$	118.0±2.9	83.5±4.8	99.8±0.4
15min AT-PDGFRβ$^+$	115.1±3.3	84.6±4.8	99.8±0.4
30min AT-PDGFRβ$^+$	117.1±2.2	84.6±4.8	99.8±0.4
P value	0.086	0.972	0.960

The mean value of the monitored mean arterial pressure, heart rate, and O_2 saturation of 6 canines were compared among each step of the procedure by using Kruskal-Wallis test. AT-PDGFRβ$^+$=adipose tissue-originated platelet-derived growth factor receptor β positive cell; 1min or 5min manitol=1 minute or 5 minutes after hyperosmolar mannitiol injection, respectively; 10min, 15min, or 30min AT-PDGFRβ$^+$=10 minutes, 15 minutes, or 30 minutes after AT-PDGFRβ$^+$ injection, respectively; MAP=mean arterial pressure (mmHg); HR=heart rate (beats/min); SpO_2=O_2 saturation(%).

Table 3. Laboratory findings at baseline, immediate post-infusion, day 1, and day 7 after AT-PDGFRβ^{+} cell infusion

	Baseline	Post-I.	Day 1	Day 7	P value
WBC,x10^{3} μL	**10.3±1.0**	**8.0±1.6**	**9.4±0.5**	**9.7±0.9**	**0.026**
Hb, g/dL	**15.6±2.0**	**11.7±2.5**	**13.8±2.0**	**14.2±1.6**	**0.051**
PLT, x10^{3} μL	**289.7±104.3**	**325.6±86.8**	**388.1±137.3**	**369.5±110.9**	**0.526**
CA, mg/dL	**10.9±1.0**	**9.0±1.1**	**9.3±1.2**	**10.0±0.7**	**0.044**
P, mg/dL	**6.4±0.5**	**6.2±0.7**	**5.8±0.6**	**5.9±0.7**	**0.568**
GLU, mg/dL	**70.7±28.4**	**77.3±26.2**	**84.0±17.6**	**97.0±9.7**	**0.234**
BUN, mg/dL	**10.7±1.7**	**8.7±2.0**	**10.7±5.1**	**10.7±5.2**	**0.797**
Creatinine, mg/dL	**1.7±1.1**	**1.3±0.4**	**1.2±0.3**	**1.3±0.1**	**0.067**
Cholesterol, mg/dL	**259.2±28.2**	**187.1±32.7**	**217.1±45.7**	**230.6±39.2**	**0.053**
Total protein, mg/dL	**6.6±0.3**	**5.1±0.5**	**5.9±0.3**	**5.8±0.3**	**0.001**
Albumin, mg/dL	**2.8±0.3**	**2.1±0.2**	**2.4±0.2**	**2.5±0.2**	**0.007**
AST, IU/L	**38.5±10.5**	**31.2±10.4**	**33.6±8.2**	**26.5±3.1**	**0.191**
ALT, IU/L	**32.7±17.3**	**18.3±11.9**	**15.3±8.8**	**15.1±9.1**	**0.113**
CK, IU/L	**205.0±39.0**	**196.8±55.2**	**230.1±81.6**	**188.1±33.5**	**0.622**
LD, IU/L	**234.0±72.5**	**184.3±107.3**	**254.6±35.4**	**201.5±81.2**	**0.446**
CRP, mg/dL	**0.04±0.00**	**0.03±0.01**	**0.03±0.01**	**0.03±0.00**	**0.371***

Na, mmol/L	**144.6±3.2**	**145.8±6.0**	**142.3±5.1**	**143.8±3.9**	**0.654**
K, mmol/L	**4.9±0.2**	**4.5±0.5**	**5.0±0.3**	**5.2±0.2**	**0.020**
Cl, mmol/L	**108.8±6.1**	**104.6±10.1**	**106.2±5.7**	**109.3±3.2**	**0.630**
PT, sec	**6.9±0.6**	**6.9±0.5**	**6.4±0.3**	**6.3±0.2**	**0.236**
aPTT, sec	**19.6±6.6**	**23.6±2.4**	**16.4±2.9**	**16.5±3.0**	**0.096**

AT-PDGFRβ^{+}=adipose tissue-originated platelet-derived growth factor receptor β positive cell; The mean value of the blood profiles of 6 canines were compared among baseline, immediately after (post-I.), day 1, and day 7 after infusion of AT-PDGFRβ^{+} by using Kruskal-Wallis test. WBC=white blood cell; Hb=Hematocrit; PLT=platelet; CA=calcium; P=phosphate; GLU=glucose; BUN=blood urea nitrogen; AST=aspartate transaminase; ALT=alanine transaminase; CK=creatine kinase; LD=lactate dehydrogenase; CRP=C-reactive protein, *CRP levels are within normal range; Na=sodium; K=potassium; Cl=chloride; PT=prothrombin time; aPTT=activated partial thromboplastin time.

Table 4. Neurologic scales of six canines after day 1, day 7, and day 28 after AT-PDGFRβ$^+$ cell infusion

	Day 1	Day 7	Day 28
Motor	**1**	**1**	**1**
Consciousness	**1**	**1**	**1**
Head turning	**0**	**0**	**0**
Circling	**0**	**0**	**0**
Hemianopsia	**0**	**0**	**0**

The neurologic scales of six canines were evaluated on the day after AT-PDGFRβ$^+$ cell infusion. The mean value was 2 throughout day 1, day 7, and day 28. AT-PDGFRβ$^+$=adipose tissue-originated platelet-derived growth factor receptor β-positive cell.

Table 5. Magnetic resonance imaging findings of six canines on the day 1 and day 7 after AT-PDGFRβ$^+$ cell infusion

	Day 1	Day 7	Incidence, %
Protocol #1			**50 %**
Canine #1	**Multifocal**	**Additional**	
Canine #2	**No infarct**	**No infarct**	
Protocol #2			**25 %**
Canine #3	**No infarct**	**No infarct**	
Canine #4	**No infarct**	**No infarct**	
Canine #5	**Single tiny**	**Disappeared**	
Canine #6	**No infarct**	**No infarct**	

AT-PDGFRβ$^+$=adipose tissue-originated platelet-derived growth factor receptor β-positive cell. In the first protocol (n=2), approximately 5 x 10^6 autologous AT-PDGFRβ$^+$ cells in 2mL of PBS was slowly injected by hand injection. In the second protocol (n=4), cell solution was dissociated with hand shaking after addition of EDTA/Trypsin. The cells were mixed with a 50 mL of normal saline plus 1,000 unit of heparin solution, and the mixture were dripped slowly using pressure bag during 10 minute.

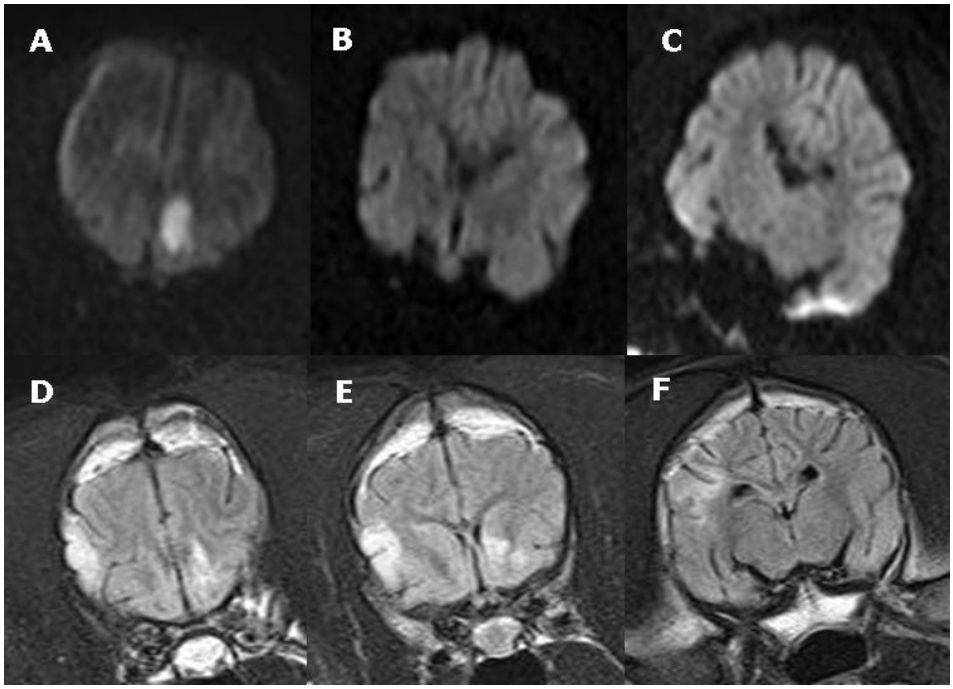

Figure 3. Brain magnetic resonance imaging of canine #1 at the day 1 and day 7 after autologous AT-PDGFRβ^{+} cell infusion

(A-C) Coronal view of diffusion-weighted imagings at 1 day after adipose tissue-originated platelet-derived growth factor receptor β-positive (AT-PDGFRβ^{+}) cells were infused via right internal carotid artery. Small areas of diffusion-restriction was found at left anterior frontal lobe contralateral to injected side at 1 day diffusion-weighted imaging. (D-F) On coronal view of fluid-attenuated inversion recovery sequence after one week, new hyperintense lesions were found at right temporoparietal lobe.

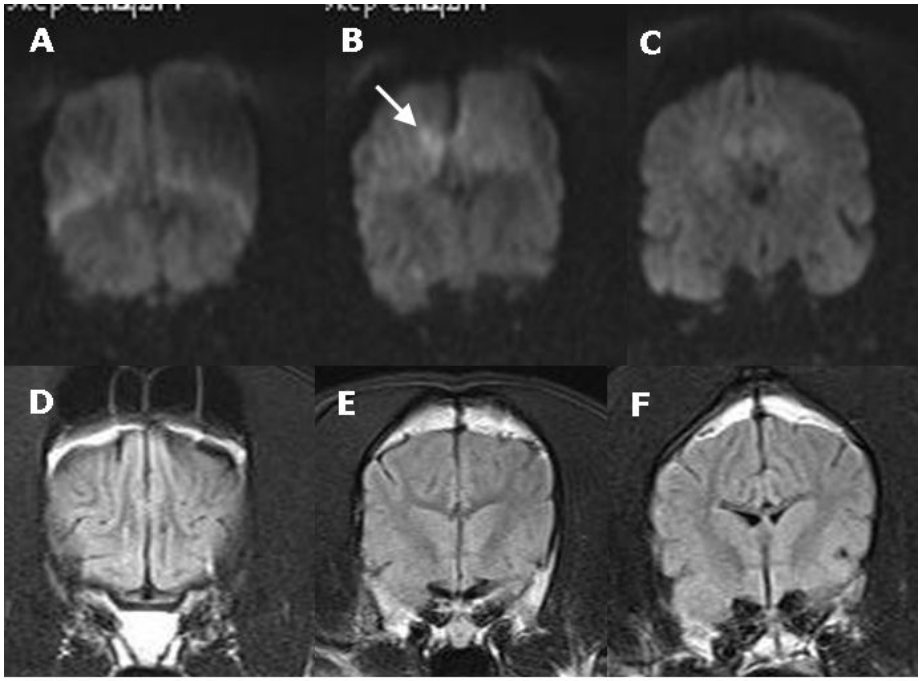

Figure 4. Brain magnetic resonance imaging of canine #5 at the day 1 and day 7 after autologous AT-PDGFRβ^{+} cell infusion

(A-C) Coronal view of diffusion-weighted imagings at 1 day after adipose tissue-originated platelet-derived growth factor receptor β-positive (AT-PDGFRβ^{+}) cells were infused via right internal carotid artery. A small diffusion-restriction lesion (arrow) was found at right frontal lobe ipsilateral to injected side. (D-F) On coronal view of fluid-attenuated inversion recovery sequence after one week, the previous diffusion-restriction disappeared and no hyperintense lesions were found.

4. Histology of transplanted autologous AT-PDGFRβ$^+$ cells within canine brain

The transplanted autologous AT-PDGFRβ$^+$ cells were detected within canine brain (Fig 5), and the location of the AT-PDGFRβ$^+$ cells was around vessel (70%), at outside vessel (20%), and within vessel (10%), regardless of protocol 1 and 2. However, the mean number of AT-PDGFRβ$^+$ cells per mm^2 at protocol 1 was higher than that at protocol 2 (0.75 cells per mm^2 versus 0.4 cells per mm^2, $p<0.001$). The AT-PDGFRβ$^+$ cells were found at both ipsilateral cortex and contralateral cortex (Fig 6), but the amount was greater in the ipsilateral hemisphere (1.25 cells per mm^2 in the ipsilateral frontal lobe versus 0.8 cells per mm^2 in the contralateral frontal lobe). The AT-PDGFRβ$^+$ cells were found most frequently in the frontal lobe followed by parietal lobe, temporal lobe, occipital lobe, and brainstem/thalamus in the ipsilateral hemisphere. The distribution pattern was similar in the contralateral hemisphere.

Even within the infracted area (Fig 7), autologous AT-PDGFRβ^{+} cells were detected, and the cell fraction of location was same between intact and infarcted brain.

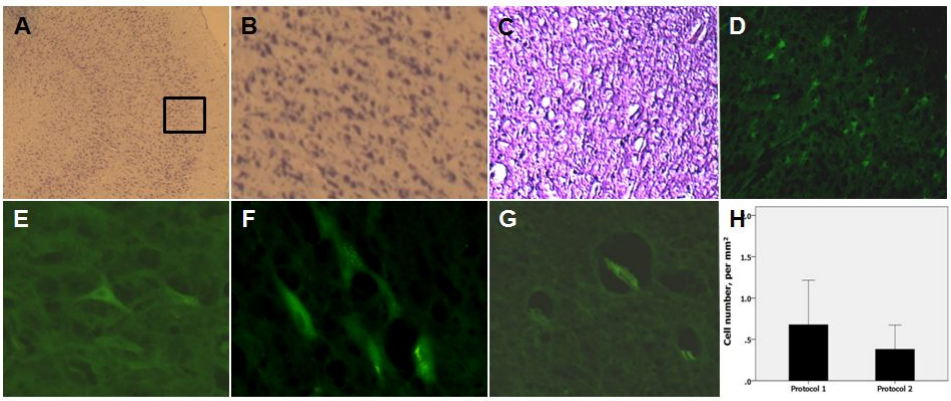

Figure 5. Detection of transplanted autologous AT-PDGFRβ$^+$ cells within canine brain

From the section of canine brain (A; cortical layer is shown inside rectangle), the cortex (B) was examined by H&E stain (C) and GFP stain (D). Regardless of protocol 1 and 2, GFP stain shows that the AT-PDGFRβ$^+$ cells are found at perivascular area (F, 70%), outside vessel (E, 20%), and within vessel (G; 10%). The mean number of AT-PDGFRβ$^+$ cells per mm^2 was greater with protocol 1 than with protocol 2 (0.75 cells per mm^2 versus 0.4 cells per mm^2, $p<0.001$).

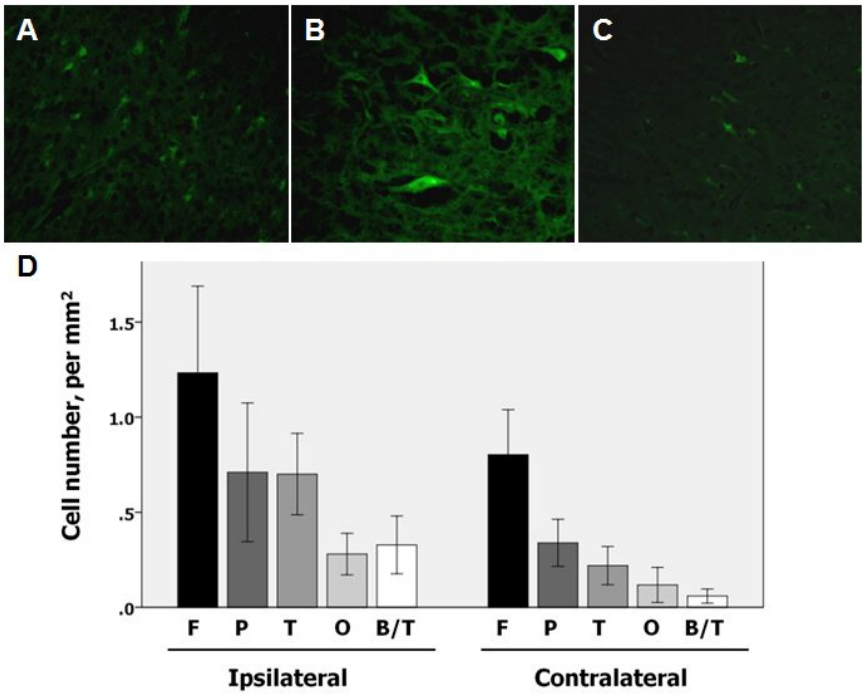

Figure 6. Geographic distribution of engrafted autologous AT-PDGFRβ$^+$ cells within canine brain

GFP stain of ipsilateral cortex (A, x100; B, x200), and contralateral cortex (C, x200) showed green engrafted AT-PDGFRβ$^+$ cells. The number of cells per mm^2 was 1.25 in the ipsilateral frontal lobe and 0.8 in the contralateral frontal lobe. The AT-PDGFRβ$^+$ cells were found most frequently in the frontal lobe followed by parietal lobe, temporal lobe, occipital lobe, and brainstem/thalamus in both ipsilateral and contralateral hemisphere.

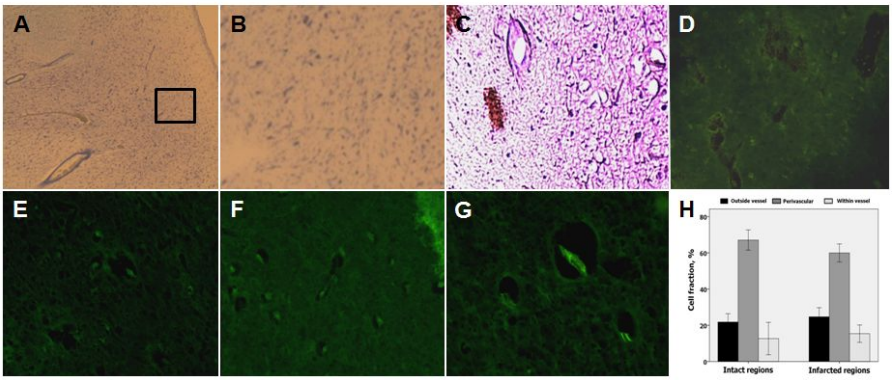

Figure 7. Detection of transplanted autologous AT-PDGFRβ^{+} cells within infracted canine brain

The infarct area of canine brain (A) showed obscuration of cortex (B, magnified view from rectangular portion of A). (C) H&E stain revealed shrunken neurons and cavitation in the ischemic cortex. On GFP stain of infarct area, the AT-PDGFRβ^{+} cells were found at outside vessel (D, 20%), around vessel (E, x100; F, x200; 70%), and within vessel (G; 10%). (H) The cell fraction of location was same between intact and infarct brain.

IV. DISCUSSION

This is the first study of demonstrating the AT-PDGFRβ$^+$ cells engraft for chronic stroke model and testing the safety of intracarotid infusion of autologous AT-PDGFRβ$^+$ cells. Pericytes have been recognized to have multipotent stem or progenitor cell-like activities in vitro (22–25), but isolation and expansion of pericytes from ATSC for cell delivery and in vivo differentiation within brain tissue have not been presented so far. In this study, the stable preparation of highly pure human AT-PDGFRβ$^+$ cells for chronic ischemic rat brain or autologous canine AT-PDGFRβ$^+$ cells for normal canine brain was successful within three weeks from adipose tissue acquisition, and their optimal medium condition was clarified, which showed an obvious feasibility of autologous AT-PDGFRβ$^+$ cell preparation toward clinical applications.

Rat and canine brain sections on day 28 showed that the surviving GFP$^+$ cells were located mainly in the perivascular space and/or

express αSMA, indicating their pericytic characteristics (23,24,30–33). In the ischemic rat brain, they differentiated mainly into endothelial cell, and some differentiated neuron, which also suggests potential of direct vascular regeneration or vasculo-neurogenesis (24). On the other hand, no astroglial differentiation of AT-PDGFRβ$^+$ cells was observed in the ischemic rat brain, which was different from basilar artery infusion of human umbilical cord blood-derived MSC (41). It might be a favorable condition of neuroregeneration in that functional reorganization would preferentially occur, but further investigation is necessary.

However, without mannitol preloading, a few AT-PDGFRβ$^+$ cells were found in the chronic ischemic rat brain after contralateral intracarotid injection. It is postulated that acute stroke already evolved to subacute stage, with losing homing signals for stem cells recruitment or BBB closure during two or three weeks required for autologous AT-PDGFRβ$^+$ preparation. The current study

demonstrated that hyperosmolar mannitol facilitated the entrance of AT-PDGFRβ$^+$ cells into chronic ischemic rat brain. AT-PDGFRβ$^+$ cells were detected in the brain tissue of chronic ischemic rat only after hyperosmolar mannitol pretreatment. Of various BBB disruption methods of mannitol pretreatment, hyperventilation, hypothermia, hypotension, and hypoperfusion (42–47), we selected mannitol pretreatment because of the easy establishment of standard protocol. Mannitol is a sugar alcohol which has been used to decrease cerebral edema or intracranial pressure (48,49), and this osmotic agent is known to open BBB by temporarily shrinking the tightly coupled endothelial cells (50), and to dilatate small vessel or capillary with improving its flow (51). The dosage of mannitol and the timing of the following AT-PDGFRβ$^+$ cell injection used in the current study were inferred from literature of cerebral enzyme and cell delivery (42,45).

The intracarotid route for AT-PDGFRβ$^+$ delivery is an attractive

approach (41), because cells could be delivered directly to the vascular territory of the affected tissue with maximizing the effectiveness of given dosage particularly in case of autologous transplantation. Intravenous injection is a simple approach, but a higher dose of stem cells would be required for clinical application (52). Local intracerebral injection is invasive and may accompany adjacent tissue damage, and multiple sessions across craniotomy may not be clinically tolerated (53).

However, arrested flow through occluded carotid artery do not deliver AT-PDGFRβ^+ cells to brain parenchyma despite hyperosmolar mannitol preloading as shown in the current study. An arterial infusion into patent contralateral carotid or basilar artery would be more permissive to enter into brain tissue, but it was still questionable whether the migration of stem cells into ischemic hemisphere would actually occur even at three weeks after stroke. The current study demonstrated that the human AT-PDGFRβ^+ cells

administered into the contralateral carotid artery migrate from non-ischemic hemisphere to ischemic hemisphere via corpus callosum. Our findings are in accord with a prior study of basilar artery injection of umbilical cord-derived stromal cells after 1 day of acute middle cerebral artery occlusion (41). The migration of transplanted cells to contralateral ischemic hemisphere suggests that chemoattractive action of rat ischemic region persists until three weeks after stroke and AT-PDGFRβ$^+$ cells respond with expression of chemokine receptor. Since the current study did not measure the serum or tissue levels of chemoattractant such as SDF-1 and the expression of chemokine receptors such as CXCR4 has not been identified in AT-PDGFRβ$^+$ cells (54–57), the detailed mechanism of AT-PDGFRβ$^+$ cell migration would be of interest as topics of future investigations.

Endovascular interventional techniques are essential for intracarotid delivery of AT-PDGFRβ$^+$ cells and applicable to animal

models larger than rodents. The canine has similar sized carotid artery to human, and the endovascular interventional techniques in canine model is well-established (58–63). A total of six normal canines of this study were evaluated by catheter angiography, vital signs, blood tests, neurohavioral score, and brain MRI to assess the safety of intracarotid injection of AT-PDGFRβ^{+} cells. Canine stroke model is beyond the scope of this study, which was not conducted in this safety testing of autologous AT-PDGFRβ^{+} cells. The vital signs were stable before and after hyperosmolar mannitiol and AT-PDGFRβ^{+} cell injection, and the laboratory tests did not show a clinically significant adverse reaction. Particularly, the CRP, the inflammatory surrogate marker was within normal range, indicating that the autologous AT-PDGFRβ^{+} cell infusion was not associated with a significant inflammatory or immunologic reaction. Although catheter angiography confirmed arterial patency in all canines, acute infarct on brain MRI was noticed in one of two canine in the

protocol 1 using concentrated cell pellet (multiple, incidence of 50%) and in one of four canines in the protocol 2 using diluted cell pellet (single tiny, incidence of 25%). On the other hand, the engrafted cell number was greater with the protocol 1 than with the protocol 2. Although the MRI-defined infarctions in this study were clinically silent and increasing engrafted cells would be preferred for a greater therapeutic effect, the thromboembolic risk of the higher cell pellet concentration should not be overlooked. Further protocol modification for an optimal balancing of the thromboembolic risk and increasing engrafted cells is necessary for human application.

The current study has several limitations. In the chronic ischemic rat model, we found that the AT-PDGFRβ^+ cells were migrated to ischemic area, but their clinical efficacy was not assessed. Because of the difficulty in quantitatively measuring the magnitude of BBB breakdown, an optimal dosage of pretreatment mannitol was not determined. In addition, an optimal amount of the AT-PDGFRβ^+ cells

was not also determined as we tested a single dosage. Given the small number of engrafted cells in the chronic ischemic rat model, the dosage escalation study needs to be performed.

V. Conclusion

In summary, the pretreatment of hyperosmolar mannitol enhanced the delivery of human AT-PDGFRβ$^+$ cells into chronic ischemic rat brain by transiently opening BBB. The contralaterally infused human AT-PDGFRβ$^+$ cells migrated via corpus callosum into the chronic ischemic rat brain and differentiated into neuronal or endothelial cells. The intracarotid injection of autologus AT-PDGFRβ$^+$ cells in the normal non-ischemic canines was not associated with significant adverse reactions except a silent thromboembolism. To overcome this complication, further improvement in cell pellet preparation is required. In conclusion, the intracarotid infusion of AT-PDGFRβ$^+$ cells under the hyperosmolar mannitiol pretreatment can be a useful cell-based neurorestorative therapy in the chronic stage of stroke.

VI. REFERENCES

1. Statistics Korea. Annual Report on the Cause of Death Statistics, 2010. Daejeon: Statistics Korea; 2011. Available from: URL: http://kostat.go.kr/portal/korea/kor_nw/2/6/2/index.board

2. Organisation for Economic Co-operation and Development (OECD). OECD Health Data 2011. Available from: URL: www.oecd.org/health/healthdata

3. World Health Organization. World Health Report 2002. Available from: URL: http://www.who.int/whr/2002/en/whr02_en.pdf

4. Dirnagl U, Iadecola C, Moskowitz MA. Pathobiology of ischaemic stroke: an integrated view. Trends Neurosci. 1999; 22: 391–7.

5. Gladstone DJ, Black SE, Hakim AM; Heart and Stroke Foundation of Ontario Centre of Excellence in Stroke Recovery. Toward wisdom from failure: lessons from neuroprotective stroke trials and new therapeutic directions. Stroke. 2002; 33: 2123–36.

6 Pittenger MF, Mackay AM, Beck SC, Jaiswal RK, Douglas R, Mosca

JD, Moorman MA, Simonetti DW, Craig S, Marshak DR. Multilineage potential of adult human mesenchymal stem cells. Science. 1999; 284: 143–7.

7. Haas S, Weidner N, Winkler J. Adult stem cell therapy in stroke. Curr Opin Neurol. 2005; 18: 59–64.

8. Guzman R, Choi R, Gera A, De Los Angeles A, Andres RH, Steinberg GK. Intravascular cell replacement therapy for stroke. Neurosurg Focus. 2008; 24: E15.

9. van Velthoven CT, Kavelaars A, van Bel F, Heijnen CJ. Regeneration of the ischemic brain by engineered stem cells: fuelling endogenous repair processes. Brain Res Rev. 2009; 61: 1–13.

10. Dharmasaroja P. Bone marrow-derived mesenchymal stem cells for the treatment of ischemic stroke. J Clin Neurosci. 2009; 16: 12–20.

11. Walker PA, Harting MT, Shah SK, Day MC, El Khoury R, Savitz SI, Baumgartner J, Cox CS. Progenitor cell therapy for the treatment of central nervous system injury: a review of the state of current clinical trials. Stem Cells Int. 2010; 20: 369578.

12. Bianco P, Riminucci M, Gronthos S, Robey PG. Bone marrow stromal stemcells: nature, biology and potential applications. Stem Cells. 2001; 19: 180–92.

13. Zhao Y, Glesne D, Huberman E. A human peripheral blood monocyte-derived subset acts as pluripotent stem cells. Proc Natl Acad Sci USA. 2003; 100: 2426–31.

14. Jung KH, Chu K, Lee ST, Song EC, Sinn DI, Kim JM, Kim SJ, Kim JH, Kang KM, Park HK, Lee SH, Kim M, Lee SK, Roh JK. Identification of neuronal outgrowth cells from peripheral blood of stroke patients. Ann Neurol. 2008; 63: 312–22.

15. Cesselli D, Beltrami AP, Rigo S, Bergamin N, D'Aurizio F, Verardo R, Piazza S, Klaric E, Fanin R, Toffoletto B, Marzinotto S, Mariuzzi L,

Finato N, Pandolfi M, Leri A, Schneider C, Beltrami CA, Anversa P. Multipotent Progenitor Cells Are Present in Human Peripheral Blood. Circ Res. 2009; 104: 1225–34

16. Koh SH, Kim KS, Choi MR, Jung KH, Park KS, Chai YG, Roh W, Hwang SJ, Ko HJ, Huh YM, Kim HT, Kim SH. Implantation of human umbilical cord-derived mesenchymal stem cells as a neuroprotective therapy for ischemic stroke in rats. Brain Res. 2008; 1229: 233–48.

17. Zuk PA, Zhu M, Mizuno H, Huang J,Futrell JW, Katz AJ, Benhaim P, Lorenz HP, Hedrick MH. Multilineage cells from human adipose tissue: implications for cell-based therapies. Tissue Eng. 2001; 7: 211–18.

18. Safford KM, Hicok KC, Safford SD,Halvorsen YD, Wilkison WO, GimbleJM, Rice HE. Neurogenic differentiation of murine and human adipose-derivedstromal cells. Biochem Biophys Res Commun. 2002; 294: 371–79.

19. Kang SK, Lee DH, Bae YC, Kim HK, Baik SY, Jung JS. Improvement of neurological deficits by intracerebral transplantation of human adipose tissue-derived stromal cells after cerebral ischemia in rats. Exp Neurol. 2003; 183: 355–66.

20. Kim JM, Lee ST, Chu K, Jung KH, Song EC, Kim SJ, Sinn DI, Kim JH, Park DK, Kang KM, Hyung Hong N, Park HK, Won CH, Kim KH, Kim M, Kun Lee S, Roh JK. Systemic transplantation of human adipose stem cells attenuated cerebral inflammation and degeneration in a hemorrhagic stroke model. Brain Res. 2007; 1183: 43–50.

21. Jung KH, Chu K, Lee ST, Bahn JJ, Jeon D, Kim JH, Kim S, Won CH, Kim M, Lee SK, Roh JK. Multipotent PDGFRβ-expressing cells in the circulation of stroke patients. Neurobiol Dis. 2011; 41: 489–97.

22. Lee RH, Kim B, Choi I, Kim H, Choi HS, Suh K, Bae YC, Jung JS. Characterization and expression analysis of mesenchymal stem cells from human bone marrow and adipose tissue. Cell. Physiol.

Biochem. 2004; 14: 311–24.

23. Farrington-Rock C, Crofts N, Doherty MJ, Ashton BA, Griffin-Jones C, and Canfield AE. Chondrogenic and adipogenic potential of microvascular pericytes. Circulation. 2004; 110; 2226–32.

24. Dore-Duffy P, Katychev A, Wang X, Van Buren E. CNS microvascular pericytes exhibit multipotential stem cell activity. J Cereb Blood Flow Metab. 2006; 26: 613–24.

25. Crisan M, Yap S, Casteilla L, Chen CW, Corselli M, Park TS, Andriolo G, Sun B, Zheng B, Zhang L, Norotte C, Teng PN, Traas J, Schugar R, Deasy BM, Badylak S, Buhring HJ, Giacobino JP, Lazzari L, Huard J, Péault B. A perivascular origin for mesenchymal stem cells in multiple human organs. Cell Stem Cell. 2008; 3: 301–13.

26. Shepro D, Morel NM. Pericyte physiology. FASEB J. 1993; 7: 1031–8.

27. Fisher M. Pericyte signaling in the neurovascular unit. Stroke. 2009; 40: S13–5.

28. Krueger M, Bechmann I. CNS pericytes: concepts, misconceptions, and a way out. Glia. 2010; 58: 1–10.

29. Kamouchi M, Ago T, Kitazono T. Brain pericytes: emerging concepts and functional roles in brain homeostasis. Cell Mol Neurobiol. 2011; 31: 175–93.

30. Schlingemann RO, Rietveld FJ, de Waal RM, Ferrone S, Ruiter DJ. Expression of the high molecular weight melanoma-associated antigen by pericytes during angiogenesis in tumors and in healing wounds. Am J Pathol. 1990; 136: 1393–405.

31. Ozerdem U, Grako KA, Dahlin-Huppe K, Monosov E, Stallcup WB. NG2 proteoglycan is expressed
exclusively by mural cells during vascular morphogenesis. Dev Dyn. 2001; 222: 218–27.

32. Tang W, Zeve D, Suh JM, Bosnakovski D, Kyba M, Hammer RE, Tallquist MD, Graff JM. White fat progenitor cells reside in the adipose vasculature. Science. 2008; 322: 583–6.

33. Traktuev DO, Merfeld-Clauss S, Li J, Kolonin M, Arap W, Pasqualini R, Johnstone BH, March KL. A population of multipotent CD34-positive adipose stromal cells share pericyte and mesenchymal surface markers, reside in a periendothelial location, and stabilize endothelial networks. Circ Res. 2008; 102: 77–85.

34. Sims DE. Recent advances in pericyte biology: implications for healthand disease. Can J Cardiol. 1991; 7: 431–43.

35. Diaz-Flores L, Gutierrez R, Varela H, Rancel N, Valladares F. Microvascular pericytes: a review of their morphological and functional characteristics. Histol Histopathol. 1991; 6: 269–86.

36. Doherty MJ, Ashton BA, Walsh S, Beresford JN, Grant ME, Canfield AE. Vascular pericytes expressosteogenic potential in vitro and in vivo. J Bone Miner Res. 1998; 13: 828–38.

37. Doherty MJ, Canfield AE. Gene expression during vascular pericyte differentiation. Crit Rev Eukaryot Gene Express. 1999; 9: 1–17.

38. Klein D, Weisshardt P, Kleff V, Jastrow H, Jakob HG, Ergün S. Vascular wall-resident CD44+ multipotent stem cells give rise to pericytes and smooth muscle cells and contribute to new vessel maturation. PLoS One. 2011; 6: e20540.

39. Purdy PD, Devous MD Sr, Batjer HH, White CL 3rd, Meyer Y, Samson DS. Microfibrillar collagen model of canine cerebral infarction. Stroke. 1989; 20: 1361–7.

40. Kang BT, Jang DP, Gu SH, Lee JH, Jung DI, Lim CY, Kim HJ, Kim YB, Kim HJ, Woo EJ, Cho ZH, Park HM. MRI features in a canine model of ischemic stroke: correlation between lesion volume and neurobehavioral status during the subacute stage. Comp Med. 2009; 59: 459–64.

41. Chung DJ, Choi CB, Lee SH, Kang EH, Lee JH, Hwang SH, Han H, Lee JH, Choe BY, Lee SY, Kim HY. Intraarterially delivered human umbilical cord blood-derived mesenchymal stem cells in canine cerebral ischemia. J Neurosci Res. 2009; 87: 3554–67.

42. Neuwelt EA, Barranger JA, Brady RO, Pagel M, Furbish FS, Quirk JM, Mook GE, Frenkel E. Delivery of hexosaminidase A to the cerebrum after osmotic modification of the blood--brain barrier. Proc Natl Acad Sci U S A. 1981; 78: 5838–41.

43. Yarnitsky D, Gross Y, Lorian A, Shalev A, Shorer S, Tanaka T, Ayajiki K, Fujimiya M, Okamura T. Increased BBB permeability by parasympathetic sphenopalatine ganglion stimulation in dogs. Brain Res. 2004; 1018: 236–40.

44. Wang M, Etu J, Joshi S. Enhanced disruption of the blood brain barrier by intracarotid mannitol injection during transient cerebral hypoperfusion in rabbits. J Neurosurg Anesthesiol. 2007; 19: 249–56.

45. Seyfried DM, Han Y, Yang D, Ding J, Savant-Bhonsale S, Shukairy MS, Chopp M. Mannitol enhances delivery of marrow stromal cells to the brain after experimental intracerebral hemorrhage. Brain Res. 2008; 1224: 12–9.

46. Joshi S, Wang M, Etu JJ, Suckow RF, Cooper TB, Feinmark SJ, Bruce JN, Fine RL. Transient cerebral hypoperfusion enhances intraarterial carmustine deposition into brain tissue. J Neurooncol. 2008; 86: 123–32.

47. Joshi S, Reif R, Wang M, Zhang J, Ergin A, Bruce JN, Fine RL, Bigio IJ. Intraarterial Mitoxantrone Delivery in Rabbits: An Optical Pharmacokinetic Study. Neurosurgery. 2011; 69: 706–12.

48. McGraw CP, Howard. Effect of mannitol on increased intracranial pressure. Neurosurgery. 1983; 13: 269–71.

49. Schwarz S, Schwab S, Bertram M, Aschoff A, Hacke W. Effects of hypertonic saline hydroxyethyl starch solution and mannitol in patients with increased intracranial pressure after stroke. Stroke. 1998; 29: 1550–5.

50. Kroll RA, Neuwelt EA. Outwitting the blood-brain barrier for therapeutic purposes: osmotic opening and other means. Neurosurgery. 1998; 42: 1083–99.

51. Burke AM, Quest DO, Chien S, Cerri C. The effects of mannitol on blood viscosity. J Neurosurg. 1981; 55: 550–3.

52. Chen J, Li Y, Wang L, Zhang Z, Lu D, Lu M, Chopp M. Therapeutic benefit of intravenous administration of bone marrow stromal cells after cerebral ischemia in rats. Stroke. 2001; 32: 1005–11.

53. Gage FH, Coates PW, Palmer TD, Kuhn HG, Fisher LJ, Suhonen JO, Peterson DA, Suhr ST, Ray J. Survival and differentiation of adult neuronal progenitor cells transplanted to the adult brain. Proc Natl Acad Sci U S A. 1995; 92: 11879–83.

54. Imitola J, Raddassi K, Park KI, Mueller FJ, Nieto M, Teng YD, Frenkel D, Li J, Sidman RL, Walsh CA, Snyder EY, Khoury SJ. Directed migration of neural stem cells to sites of CNS injury by the stromal cell-derived factor 1alpha/CXC chemokine receptor 4 pathway. Proc Natl Acad Sci U S A. 2004; 101: 18117–22.

55. Wang Y, Deng Y, Zhou GQ. SDF-1alpha/CXCR4-mediated migration of systemically transplanted bone marrow stromal cells towards ischemic brain lesion in a rat model. Brain Res. 2008; 1195: 104–12.

56. Stellos K, Langer H, Daub K, Schoenberger T, Gauss A, Geisler T, Bigalke B, Mueller I, Schumm M, Schaefer I, Seizer P, Kraemer BF, Siegel-Axel D, May AE, Lindemann S, Gawaz M. Platelet-derived stromal cell-derived factor-1 regulates adhesion and promotes differentiation of human CD34+ cells to endothelial progenitor cells. Circulation. 2008; 117: 206–15.

57. Ryu CH, Park SA, Kim SM, Lim JY, Jeong CH, Jun JA, Oh JH, Park SH, Oh WI, Jeun SS. Migration of human umbilical cord blood mesenchymal stem cells mediated by stromal cell-derived factor-1/CXCR4 axis via Akt, ERK, and p38 signal transduction pathways. Biochem Biophys Res Commun. 2010; 398: 105–10.

58. Shaibani A, Khawar S, Shin W, Cashen TA, Schirf B, Rohany M,

Kakodkar S, Carroll TJ. First results in an MR imaging--compatible canine model of acute stroke. AJNR Am J Neuroradiol. 2006; 27: 1788–93.

59. Levy EI, Hanel RA, Tio FO, Garlick DS, Bailey L, Cunningham MR, Williard C, Sherman D, Dooley JF, Kopia GA. Safety and pharmacokinetics of sirolimus-eluting stents in the canine cerebral vasculature: 180 day assessment. Neurosurgery. 2006; 59: 925–33.

60. Harris AD, Kosior JC, Ryder RC, Andersen LB, Hu WY, Hudon M, Morrish WH, Sevick RJ, Wong J, Frayne R. MRI of ischemic stroke in canines: applications for monitoring intraarterial thrombolysis. J Magn Reson Imaging. 2007; 26: 1421–8.

61. Harris AD, Kosior RK, Chen HS, Andersen LB, Frayne R. Evolution of hyperacute stroke over 6 hours using serial MR perfusion and diffusion maps. J Magn Reson Imaging. 2009; 29: 1262–70.

62. Bley T, Strother CM, Pulfer K, Royalty K, Zellerhoff M,

Deuerling-Zheng Y, Bender F, Consigny D, Yasuda R, Niemann D. C-arm CT measurement of cerebral blood volume in ischemic stroke: an experimental study in canines. AJNR Am J Neuroradiol. 2010; 31: 536–40.

63. Christoforidis GA, Rink C, Kontzialis MS, Mohammad Y, Koch RM, Abduljalil AM, Bergdall VK, Roy S, Khanna S, Slivka AP, Knopp MV, Sen CK. An endovascular canine middle cerebral artery occlusion model for the study of leptomeningeal collateral recruitment. Invest Radiol. 2011; 46: 34–40.

백서와 개모델에서 지방조직유래 혈소판성장인자 베타수용체 양성 세포의 경동맥 주입 방법 연구: 고장성 만니톨 주입으로 유도된 혈액-뇌장벽 해제 후 세포 전달의 유용성

국문초록

지방조직유래 기질세포에서 분리된, 혈소판유래성장인자 베타수용체를 가진 혈관주위세포 (AT-PDGFRβ$^+$세포)는 다가능성 중배엽 줄기세포로서, 이를 이용한 세포기반의 신경재생치료가 기대된다. 본 연구는 만성뇌졸중을 유도한 백서 모델에서 AT-PDGFRβ$^+$세포를 경동맥으로 주입할때, 고장성의 만니톨에 의해 세포전달의 효율성이 증진되는지, 또한 반대측 경동맥으로 주입된 AT-PDGFRβ$^+$세포가 뇌경색 반구에 도달하여 신경원세포 또는 혈관내피세포로 분화하는지 알아보고자 하였다. 또한 정상 개에서 고장성 만니톨과 자가 AT-PDGFRβ$^+$세포의 안전성을 확인하고자 하였다. 백서에서 만성뇌졸중이 유도된 뒤 3주후에, 1.4M 만니톨 (2mL, 0.1mL/sec)과 2x10^{6}개의 인간 AT-PDGFRβ$^+$세포를 반대측 경동맥으로 주입하는

만니톨사용군 (n=9)과 2mL 멸균 PBS와 $2x10^6$개의 인간 AT-PDGFRβ$^+$세포를 주입하는 대조군 (n=6)으로 구분하였다. 만니톨사용군에서 AT-PDGFRβ$^+$세포는 주입 3일째 비경색 반구와 뇌량에서, 주입 7일째 경색 반구에서 발견되었다. 그러나 만니톨 전처치없이 반대측 경동맥으로 주입한 경우 7일째 뇌경색 부위에서 관찰되는 AT-PDGFRβ$^+$세포는 거의 없었다. 28일째 AT-PDGFRβ$^+$세포는 뇌경색 반구의 혈관주위 공간에 주로 위치하였으며 EBA (~65%), αSMA (~40%) 또는 NF (~20%)로 염색되었다. 정상 개 (25kg, n=6)에서 고장성 만니톨 (20%, 50mL, 1g/kg)과 $5x10^6$개의 자가 AT-PDGFRβ$^+$세포를 경동맥을 통해 주입하였다. 첫번째 프로토콜 (n=2)에서, 세포를 2mL의 생리식염수에 혼합하여 1분동안 손으로 주입하였다. 두번째 프로토콜 (n=4)에서, 50mL 생리식염수, 1,000 단위의 헤파린, 세포용액으로 구성된 혼합액을 10분 동안 천천히 점적하였다. 각각의 시술단계에서 평균동맥압, 맥박수, 산소포화도는 변화 없었다. 혈액검사에서 백혈구 개수, 혈색소 수치, 칼슘, 칼륨, 알부민 및 전단백질 수치가 기준치에 비해 시술후 감소하였으나 다른 혈구 개수, 전해질, 간 및 콩팥 지수, 염증지수는 정상 범위였다. 6마리 개

모두에서 신경학적 결손이 없고 연속된 혈관조영에서 동맥의 개방성을 보였으나, 뇌자기공명영상에서 군데군데 여러 개의 (프로토콜 1; 2마리 중 한마리) 또는 작고 일시적인 단일 (프로토콜 2; 4마리 중 한마리) 병변이 관찰되었다. 개의 뇌절편에서 동측과 반대측 반구 피질 모두에서 AT-PDGFRβ^{+}세포가 발견되었으며, 특히 동측 반구와 전두엽에 좀더 빈번하게 발견되었다. 뇌경색 부위에서도 AT-PDGFRβ^{+}세포가 발견되었으며, 뇌경색 부위 여부에 무관하게 혈관주위공간 (70%), 혈관바깥쪽 (20%), 그리고 혈관안쪽 (10%)에서 관찰되었다. 요약하면, 고장성 만니톨은 백서의 만성뇌졸중 모델에서 혈액-뇌장벽을 일시적으로 열어줌으로써 반대측 경동맥에서 주입된 인간 AT-PDGFRβ^{+}세포가 혈액-뇌장벽 내부로 들어갈수 있게 하며, 뇌량을 건너 허혈반구로 이주하고 신경원 세포나 내피세포로 분화할 수 있도록 한다. 정상 개에서 자가 AT-PDGFRβ^{+}세포의 경동맥 주입은 무증상 혈전색전증 이외에는 유의한 부작용은 없지만, 이 부작용을 극복하기 위해서는 세포용액의 농도를 세심하게 변형할 것이 추천된다. 결론적으로 고장성 만니톨의 전처치후 AT-PDGFRβ^{+}세포의 경동맥 주입은 만성뇌졸중의 세포기반 신경재생치료에서 유용한 치료전략이 될 수 있다.

주 요 어 : 혈관주위세포, 지방조직유래 혈소판성장인자 베타수용체 양성세포,

만성허혈, 백서, 개, 경동맥 주입, 고장성 만니톨, 혈액-뇌장벽

학 번 : 2005-30694